Supplementary Materials

Synergistic regulation of color and mechanical properties of silicon nitride ceramics via engineering hollow structures of Eu-enriched secondary phases

Ning Liu[1,2,3], Tengfei Hu[4], Zhengqian Fu[4], Jingxian Zhang[3], Yusen Duan[3], Zhen Wang[1], Fangfang Xu[4], Shaoming Dong[1,3]

[1]Engineering & Technology Center for Aerospace Materials, Wuzhen Laboratory, Jiaxing 314500, Zhejiang, China.

[2]School of Materials Science and Engineering, Shaanxi Normal University, Xi'an 710119, Shaanxi, China.

[3]Key Laboratory of Advanced Structural Ceramics and Ceramics Matrix Composites, Shanghai Institute of Ceramics, Chinese Academy of Sciences, Shanghai 200050, China.

[4]Analysis and Testing Center for Inorganic Materials, Shanghai Institute of Ceramics, Chinese Academy of Sciences, Shanghai 200050, China.

Correspondence to: Dr. Tengfei Hu, Analysis and Testing Center for Inorganic Materials, Shanghai Institute of Ceramics, Chinese Academy of Sciences, 1295 Dingxi Road, Shanghai 200050, China. E-mail: hutf@ucas.ac.cn; Prof. Jingxian Zhang, Key Laboratory of Advanced Structural Ceramics and Ceramics Matrix Composites, Shanghai Institute of Ceramics, Chinese Academy of Sciences, 1295 Dingxi Road, Shanghai 200050, China. E-mail: jxzhang@mail.sic.ac.cn

This word file includes:

Sections 1 to 13
Figures 1 to 13
References

Section S1. Performance comparison

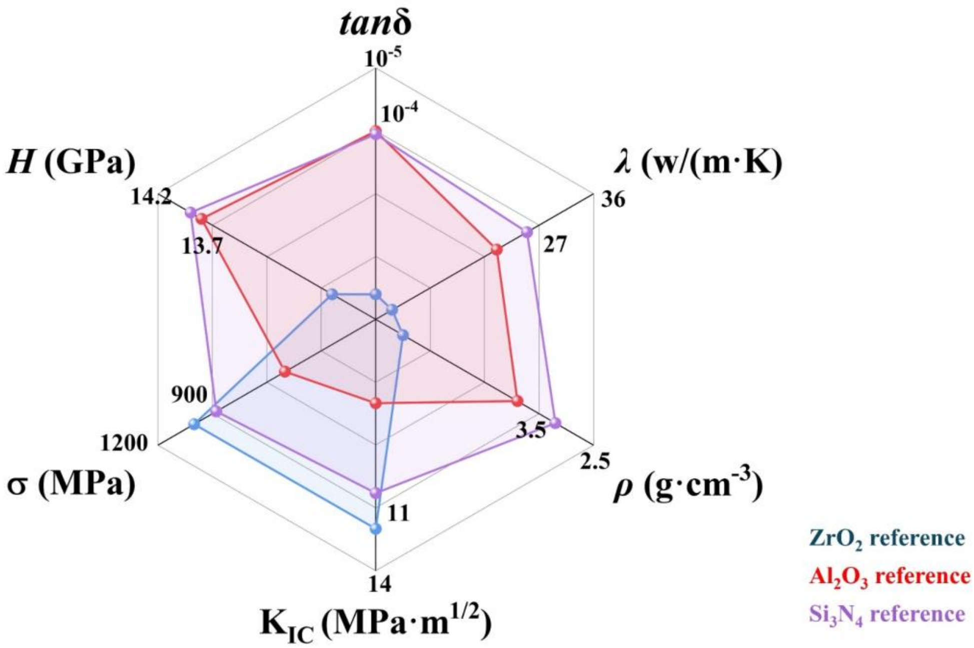

Figure 1. Physical performance of different ceramic materials. The dielectric loss (*tanδ*), thermal conductivity (λ), density s (ρ), fracture toughness (K_{IC}), flexural strength (σ) and hardness (H) of referenced ZrO_2 ceramics [1-9], referenced Al_2O_3 ceramics [10] and referenced Si_3N_4 ceramics [11-25] plotted as a radar map: The performance of Si_3N_4 ceramics is outstanding.

Section 2. Phase composition of the synthesized powder

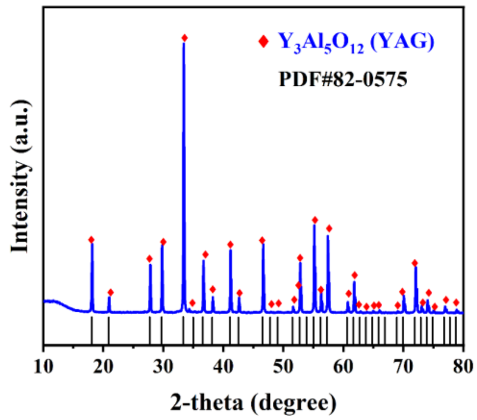

Figure 2. The XRD pattern of synthesized YAG powder.

Section 3. The glass phase separation in the grain boundary liquid phase

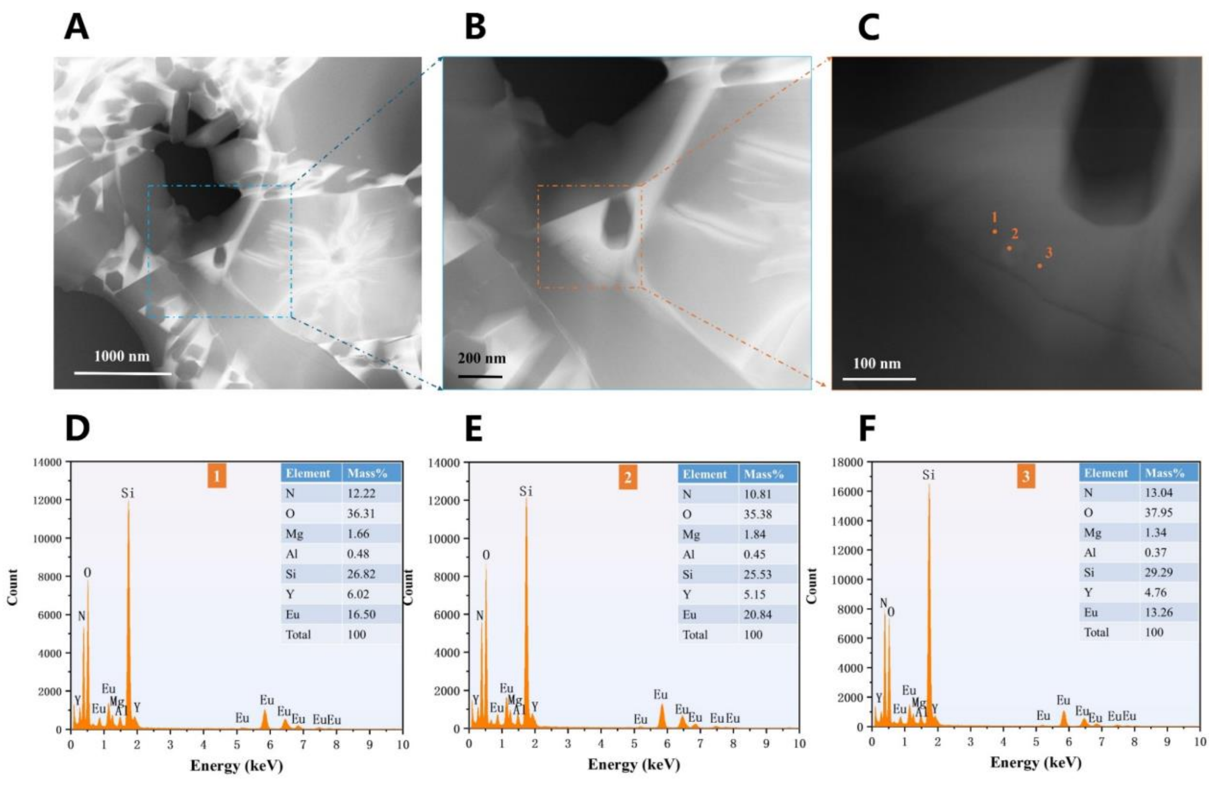

Figure 3. The STEM-EDS analysis of the regions 1-3 in grain boundary glass phase of the sample SEu-5: The hollow structure (region 2) has a higher Eu content compared to the surrounding liquid phase (region 1 and region 3).

Section 4. Micromorphology of Si_3N_4 ceramics

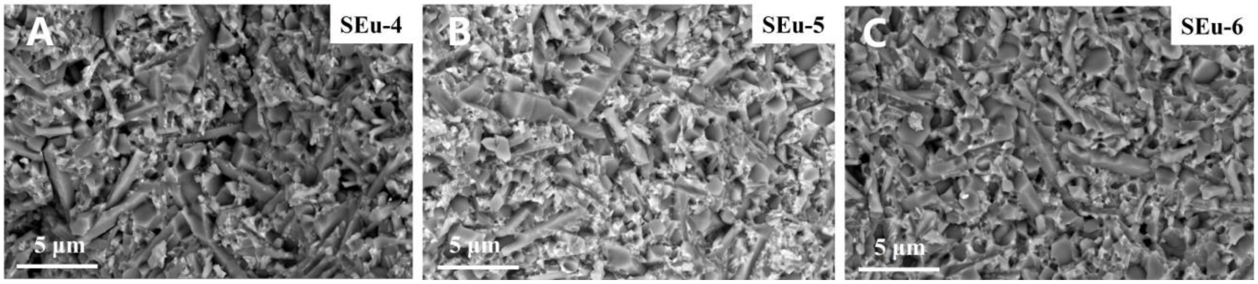

Figure 4. SEM images of the sample SEu-4 (A), SEu-5 (B) and SEu-6 (C).

Section 5. Morphology and distribution of hollow structures

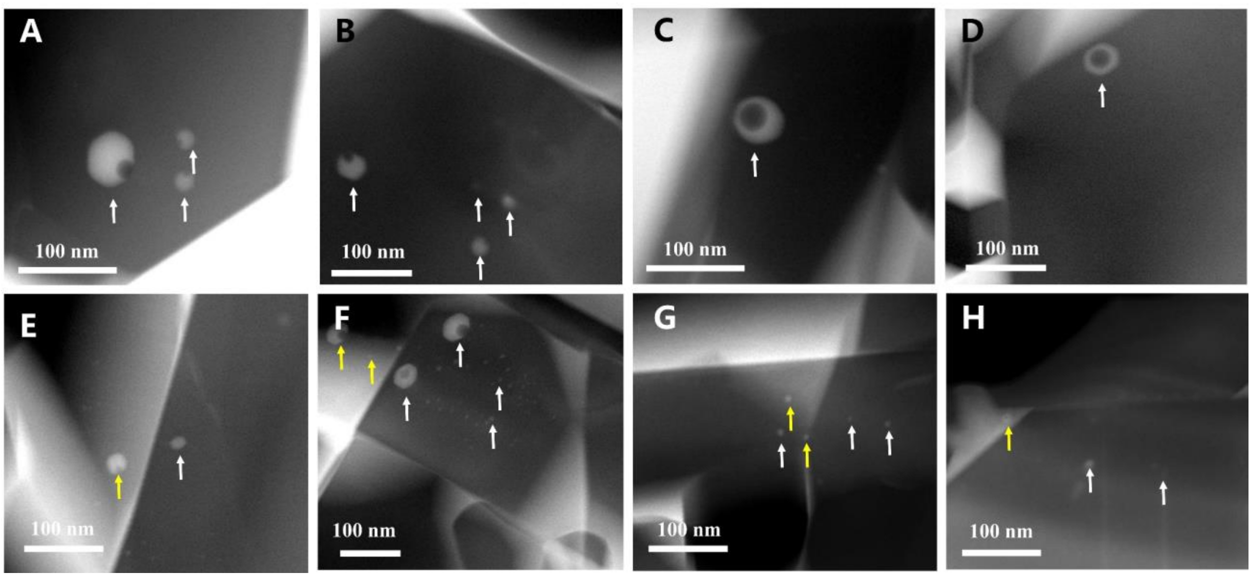

Figure 5. Distribution of hollow structures in Eu-doped Si_3N_4 ceramics. (**A-H**) STEM images of hollow structures distributed in the silicon nitride grains (white up arrows) and grain boundary glass phase: (A, E) the sample SEu-4; (B, F) the sample SEu-5; (C, G) the sample SEu-6; (D, H) the sample SEu-7.

Section 6. Diameters of hollow structures

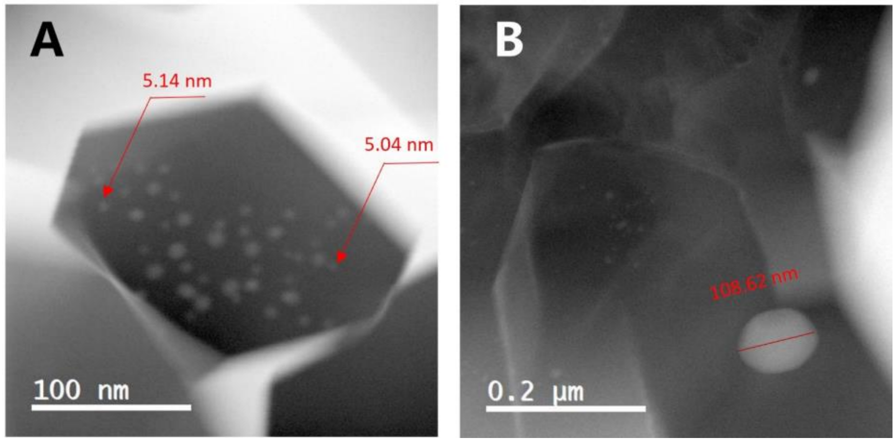

Figure 6. STEM images of the sample SEu-5 (the red line marks the diameter of the hollow structure).

Section 7. Crystallographic feature of the hollow structures

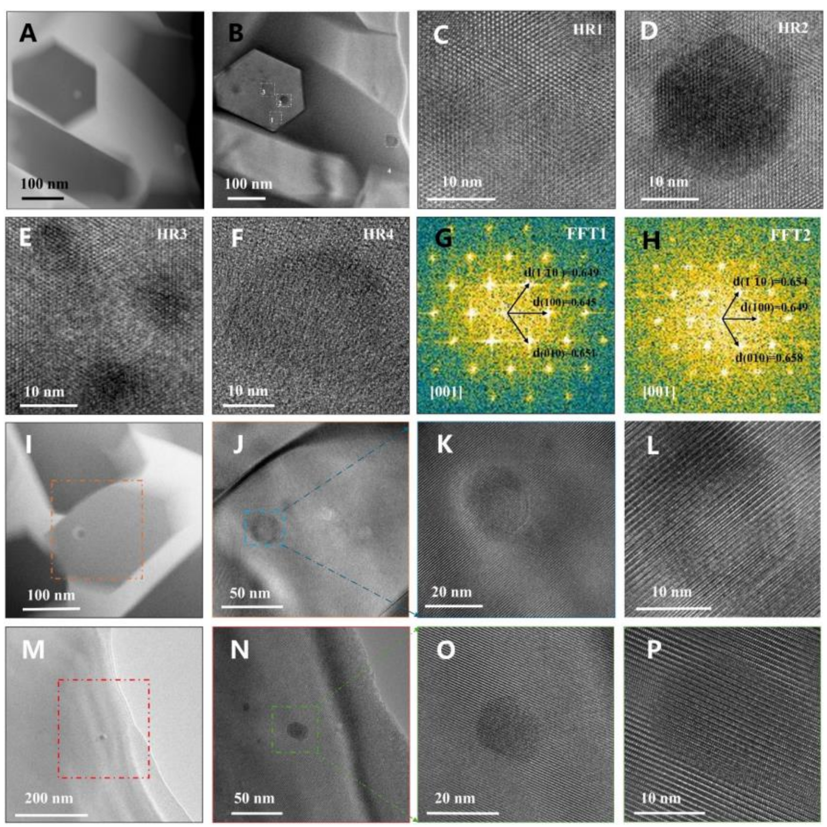

Figure 7. The structure of the hollow structure. (A) STEM image of hollow structures in the sample SEu-5; (B) TEM image corresponding to the STEM image; (C-F) HRTEM images corresponding to the region 1-4: The hollow structure has a hexahedral crystalline morphology; (G-H) FFT pattern corresponding to the HRTEM images; (I-P) STEM-HRTEM images of the hollow structure in β grains: The hollow structure in β-grain has the same hexahedral morphology as the β-grains.

Section 8. Phase composition of bulk ceramics

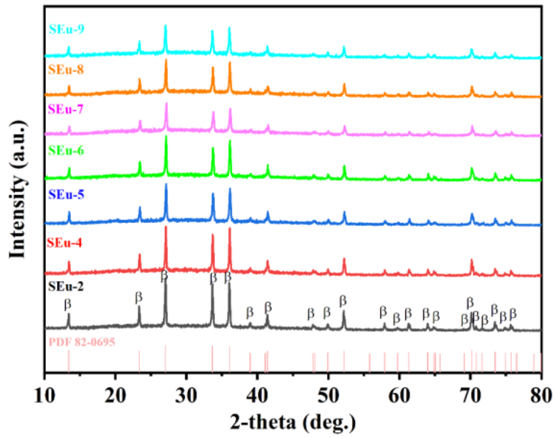

Figure 8. X-ray diffraction (XRD) analyses of all samples: The phase composition of all samples contained only the β-Si_3N_4 crystal phase, and no other crystal phase was found.

Section 9. Chemical information of the hollow structures

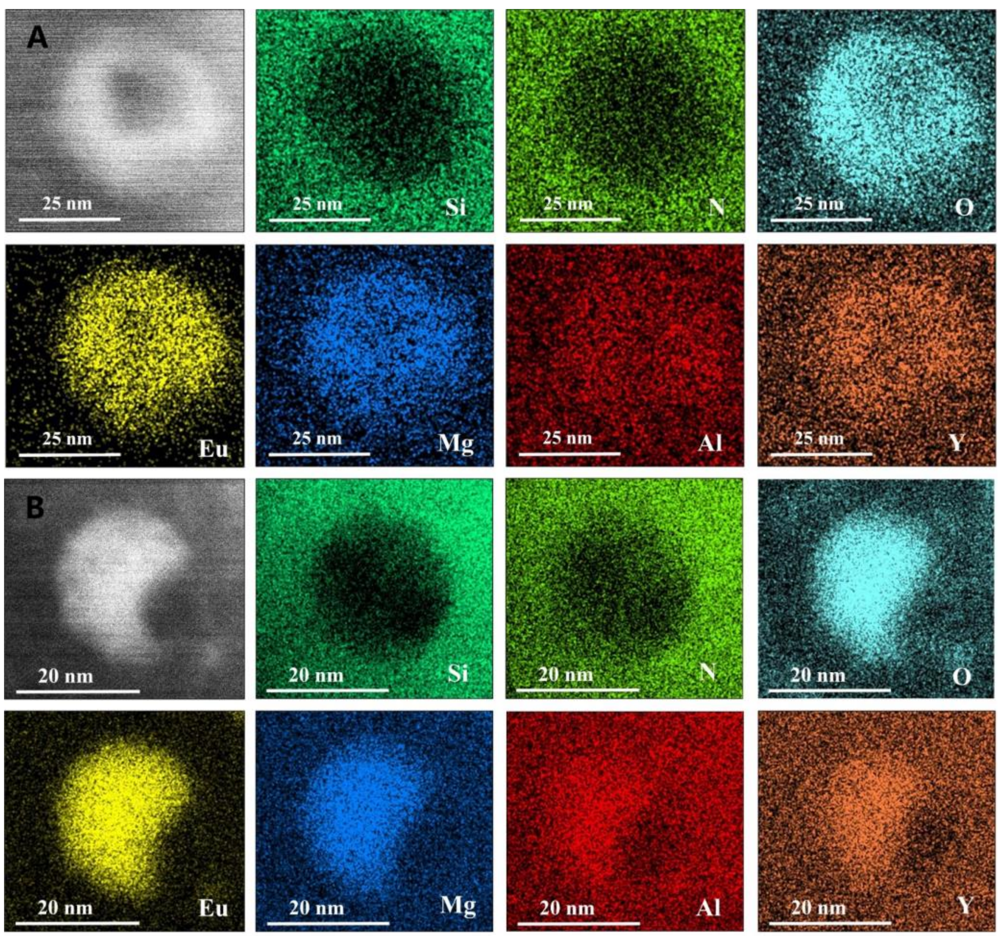

Figure 9. Element distribution in the hollow structure. (**A-B**) STEM-EDS elemental maps of the sample SEu-5.

Section 10. Valence state analysis of Eu ion

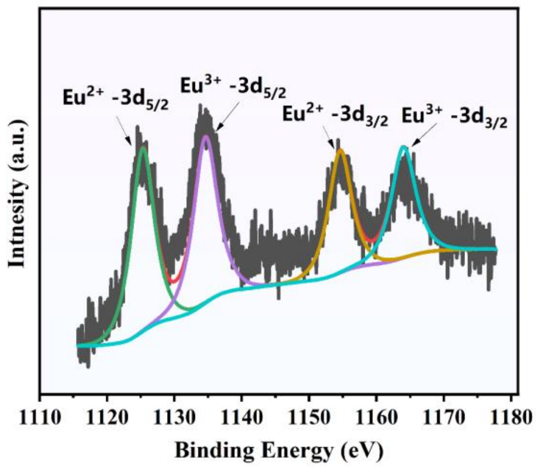

Figure 10. XPS spectrum of Eu element in the sample SEu-5. In sample SEu-5, Eu ions have two valence states, namely Eu^{2+} and Eu^{3+}.

Section 11. Physical properties

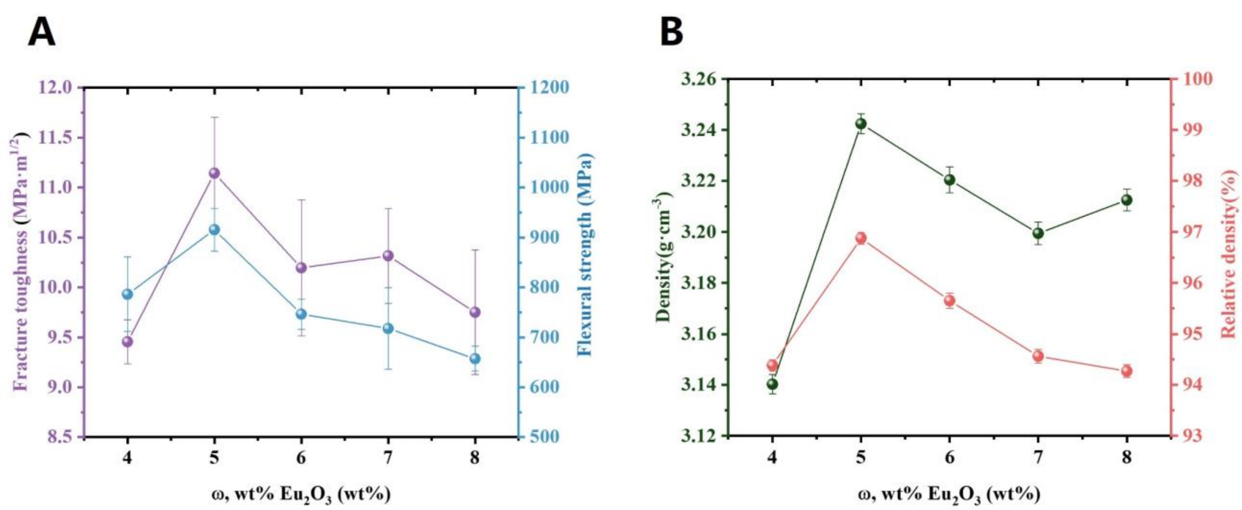

Figure 11. Physical properties of Si_3N_4 ceramics with different Eu_2O_3 contents. (**A**) The fracture toughness and flexural strength; (**B**) The density and relative density.

Section 12. Microstructures of the Si_3N_4 ceramics

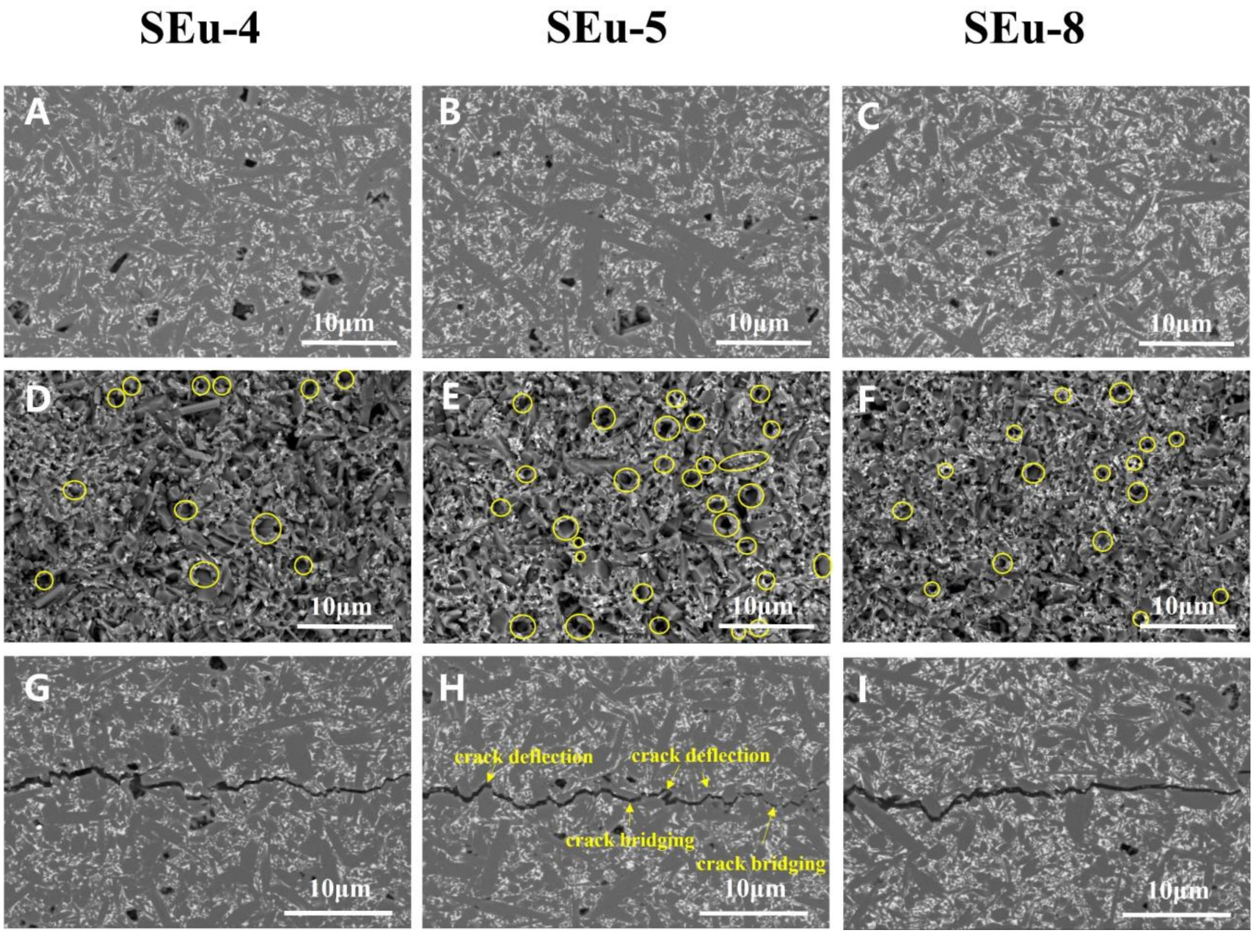

Figure 12. SEM images with BEC of the polished surfaces and fracture surfaces of the samples SEu-4 (A) (D) (G), SEu-5 (B) (E) (H) and SEu-8 (C) (F) (I) (the yellow circle marks the grain pull-out): The microstructures of the sample SEu-5 show more elongated grains, grains pull-out and curved crack growth paths, which is conducive to the consumption of crack energy and the improvement of mechanical properties [26-29].

Section 13. Intergranular fracture

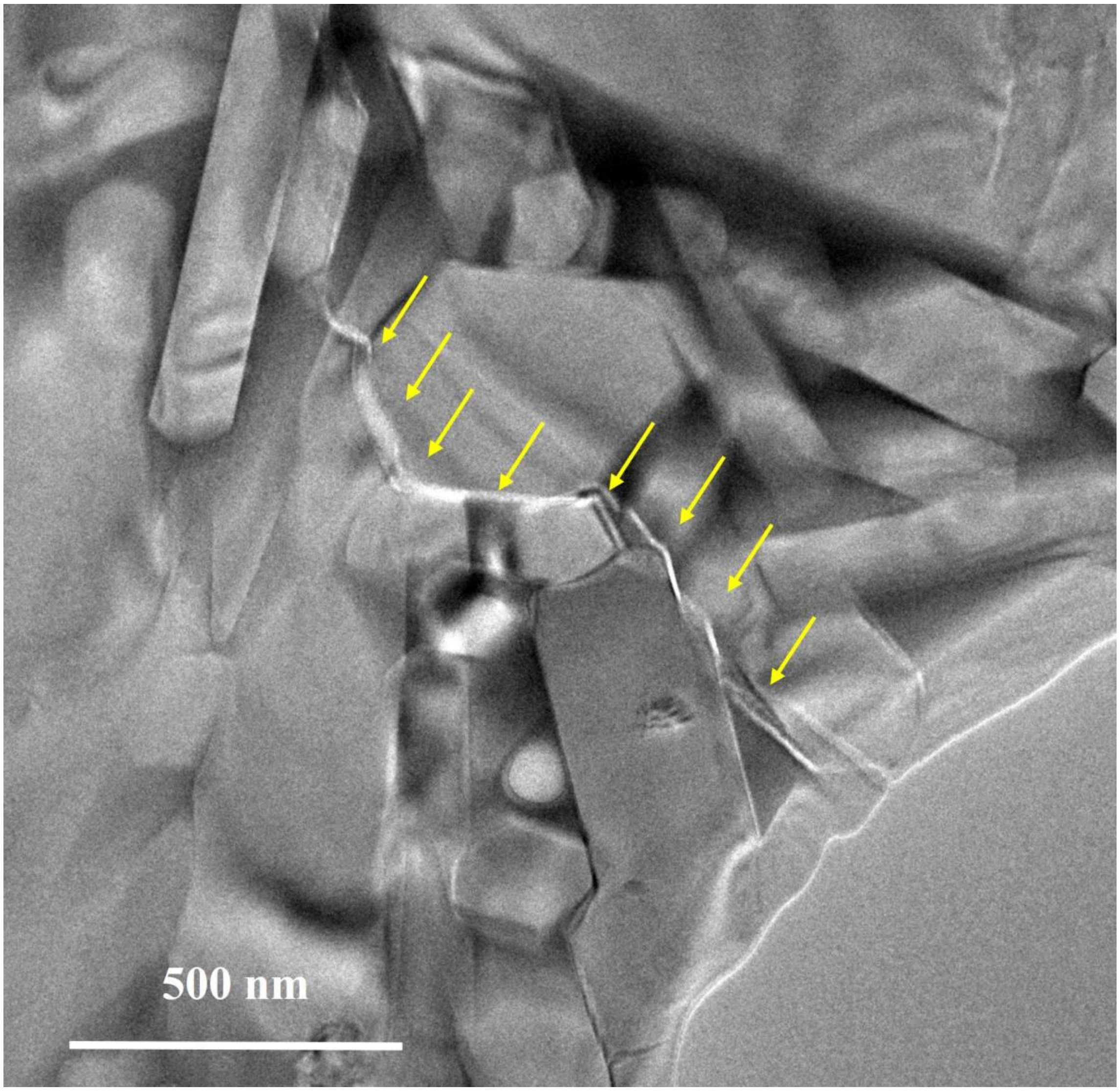

Figure 13. TEM image of crack propagation path of the sample SEu-5: Obvious intergranular fracture can be observed.

References

[1] X., et al. Thermal stability of lanthanum zirconate plasma-sprayed coating. *J. Am. Ceram. Soc* 2004; 84: 2086-2090. [DOI: 10.1111/j.1151-2916.2001.tb00962.x]

[2] Singh J, Wolfe DE, Miller RD, Eldridge J, Zhu DM. Thermal conductivity and thermal stability of zirconia and hafnia based thermal barrier coatings by EB-PVD for high temperature applications. *Materials ence Forum* 2004; 455-456: 579-586. [DOI: 10.4028/www.scientific.net/MSF.455-456.579]

[3] Peng L, Luo F, Wang X, Zhou W, Zhu D. Effect of Y_2O_3 content on microwave dielectric properties of zirconia ceramics. *Rare Metal Mat Eng* 2007; 36: 623-626. [DOI: 10.1134/S0033173207050153]

[4] Sekhar PK, Subramaniyam K, Karacolak T, Asili M, Seran S. Investigating Electromagnetic Properties of Yttria-Stabilized Zirconia (YSZ) for Wireless Gas Sensor Applications. *ECS Transactions* 2013; 53:13-19. [DOI: 10.1149/05318.0013ecst]

[5] Song Y, Zhao X, Wang A, Xiong Y, Dong Y, Wang W. Preparation and Mechanical Properties of Zirconia Ceramics Doped with Different Y_2O_3 Contents. *J Wuhan Univ Technol* 2023; 38(6):1287-1292. [DOI:10.1007/s11595-023-2821-2]

[6] Matsui K, Hosoi K, Feng B, Yoshida H, Ikuhara Y. Ultrahigh toughness zirconia ceramics. *PNAS* 2023; 120(27):2304498120. [DOI:10.1073/pnas.2304498120]

[7] Basu B. Toughening of yttria-stabilised tetragonal zirconia ceramics. *Int Mater* 2005; 50(4):239-256. [DOI: 10.1179/174328005X41113]

[8] Imariouane M, Saâdaoui M, Denis G, Reveron H, Chevalier J. Low-yttria doped zirconia: Bridging the gap between strong and tough ceramics. *J Eur Ceram Soc* 2023; 43(11): 4906-4915. [DOI: 10.1016/j.jeurceramsoc.2023.04.021]

[9] Jiang W, Lu H, Chen J, Liu X, Liu C, Song X. Toughening cemented carbides by phase transformation of zirconia. *Mater Design* 2021; 202: 109559. [DOI: 10.1016/j.matdes.2021.109559]

[10] Koller A. Structure and properties of ceramics. *Imperial College London* 1994; 11:24-27. [DOI: US2938584 A]

[11] Tapaszto, OrsolyaPuchy, ViktorHorvath, et al. The effect of graphene nanoplatelet thickness on the fracture toughness of Si_3N_4 composites. *Ceram. Int* 2018; 45: 6858-6862. [DOI: 10.1016/j.ceramint.2018.12.180]

[12] Lu X, Ning XS, Xu W, Zhou HP, Chen KX. Study on Thermal Conductivity of SPS-Sintered Si3N4 Ceramics after Heat-Treatment. *Materials Science Forum* 2005; 475-479: 1279-1282. [DOI: 10.1016/j.jeurceramsoc.2021.07.035]

[13] Chen HB, Wang W, Yu X, et al. The effect of annealing temperature on flexural strength, dielectric loss and thermal conductivity of Si_3N_4 ceramics. *J. Alloys Compd* 2020; 813: 152203-152203. [DOI: 10.1016/j.jallcom.2019.152203]

[14] Hirao K, Ohashi M, Brito ME, Kanzaki S. Processing strategy for producing highly anisotropic ssilicon nitride. *J. Am. Ceram. Soc* 1995; 78: 1687-1690. [DOI: 10.1111/j.1151-2916.1995.tb08871.x]

[15] Sun EY，Becher PF，Plucknett KP, et al. Microstructural design of silicon nitride with improved fracture toughness: II, effects of yttria and alumina additives. *J. Am. Ceram. Soc* 1998; 81: 2831-2840. [DOI: 10.1111/j.1151-2916.1998.tb02703.x]

[16] Kitayama M, Hirao K, Tsuge A, Watari K, Toriyama M, Kanzaki S. Thermal conductivity of β-Si3N4: II, effect of lattice oxygen. *J. Am. Ceram. Soc* 2000; 83: 1985-1992. [DOI: 10.1111/j.1151-2916.2000.tb01501.x]

[17] Hayashi H, Hirao K, Toriyama M, Kanzaki S, Itatani K. $MgSiN_2$ Addition as a means of increasing the thermal conductivity of β-silicon nnitride. *J. Am. Ceram. Soc* 2001; 84: 3060-3062. [DOI: 10.1111/j.1151-2916.2001.tb01141.x]
[18] Yokota H, Ibukiyama M. Microstructure tailoring for high thermal conductivity of β-Si_3N_4 ceramics. *J. Am. Ceram. Soc* 2003; 86: 197-199. [DOI: 10.1111/j.1151-2916.2003.tb03305.x]
[19] Park MK, Kim HN, Lee KS, et al. Effect of microstructure on dielectric properties of Si_3N_4 at microwave frequency. *Key Engineering Materials* 2005; 287: 247-252. [DOI: 10.4028/www.scientific.net/KEM.287.247]
[20] Xinwen, Zhu, You, Zhou, Kiyoshi, Society H. Effect of sintering additive composition on the processing and thermal conductivity of sintered rreaction-bonded Si_3N_4. *J. Am. Ceram. Soc* 2005; 87: 1398-1400. [DOI: 10.1111/j.1151-2916.2004.tb07747.x]
[21] H. Miyazaki, Y.I. Yoshizawa, K. Hirao, Fabrication of high thermal-conductive silicon nitride ceramics with low dielectric loss, Materials Science & Engineering B 161(1-3) (2009) 198-201.
[22] Hiroyuki, Miyazaki, Kiyoshi, Hirao, Yu-ichi, Yoshizawa. Effects of MgO addition on the microwave dielectric properties of high thermal-conductive silicon nitride ceramics sintered with ytterbia as sintering additives. *J Eur Ceram Soc* 2012; 32: 3297-3301. [DOI: 10.1016/j.jeurceramsoc.2012.04.025]
[23] Wang L, et al. New route to improve the fracture toughness and flexural strength of Si_3N_4 ceramics by adding $FeSi_2$. Scr. Mater; 2017: 126, 11-14. [DOI: 10.1016/j.scriptamat.2016.08.012]
[24] Wang, W, Yao, D, Liang, H, et al. Effect of the binary nonoxide additives on the densification behavior and thermal conductivity of Si_3N_4 ceramics. *J. Am. Ceram. Soc* 2020; 103: 5891-5899. [DOI: 10.1111/jace.17282]
[25] Ning L, Jza C, Ydac D, Xla C, Sda C. Effect of rare earth oxides addition on the mechanical properties and coloration of silicon nitride ceramics. *J Eur Ceram Soc* 2020; 40: 1132-1138. [DOI: 10.1016/j.jeurceramsoc.2019.11.058]
[26] Becher PF. Microstructural design of toughened ceramics. *J. Am. Ceram. Soc* 1991; 74: 255-269. [DOI: 10.1111/J.1151-2916.1991.TB06872.X]
[27] Hirosaki N, Okada A, Matoba K. Sintering of Si_3N_4 with the addition of rare-earth oxides. *J. Am. Ceram. Soc* 1988; 71: C-144-C-147. [DOI: 10.1111/j.1151-2916.1988.tb05036.x]
[28] Mitomo M, Uenosono S. Microstructural development during gas-pressure sintering of α-silicon nitride. *J. Am. Ceram. Soc* 1992; 75: 103-107. [DOI: 10.1111/j.1151-2916.1992.tb05449.x]
[29] Kawashima T, Okamoto H, Yamamot H, Kitamura A. Grain size dependence of the fracture toughness of silicon nitride ceramics. *J. Ceram. Soc. Japan* 1991; 99: 320-323. [DOI: 10.2109/jcersj.99.320]